PCCP

Accepted Manuscript

ROYAL SOCIETY OF CHEMISTRY

www.rsc.org/pccp

PCCP

RSCPublishing

Paper

Electronic structure and photoelectron spectra of B_n with n = 26 – 29. An overview of structural characteristics and growth mechanism of boron clusters

Cite this: DOI: 10.1039/x0xx00000x

Received 00th January 2014,
Accepted 00th January 2014

DOI: 10.1039/x0xx00000x

www.rsc.org/

Truong Ba Tai* and Minh Tho Nguyen*

Boron clusters are of great interest over the last decades due to their unique chemical and physical properties. In the present work, we performed a theoretical study of geometrical and electronic structure of boron clusters B_n with n = 26 – 29in both neutral and anionic states using DFT and MO computational methods. The photoelectron spectra of anionic species were simulated using TDDFT methods. Our results predict that at the neutral state both the B_{26} and B_{27} clusters exhibit tubular forms, whereas the larger species B_{28} and B_{29} are quasi-planar structures. The anionic species B_n^- are more favourable for 2D shapes. More importantly, based on the geometrical characteristics of known boron clusters, we now establish a general growth mechanism of boron clusters, which gives us more insight into the formation and existence of boron based nanomaterials.

Introduction

Stimulated by the unique properties of all-carbon nanomaterials such as graphene sheet, carbon nanotubes and fullerenes, all-boron nanomaterials have been of great interest during the past several decades. The pure boron nanotubes recently synthesized by Ciuparu*et al*.[1] and Liu *et al*.[2] marked an important breakthrough and it is expected that other B-based materials will be experimentally found in near future. Although still being a challenge for experimental studies, the cage-like structures B_{80},[3,4] and all-boron nanosheets[5,6,7] have received much attention from scientists because they form promising materials for many important applications such as the capture and storage of industrial gases (like hydrogen and carbon dioxide).

On the other hand, atomic clusters of boron are intriguing subjects, in part due to their unique characteristics of electronic structure, aromaticity and bonding nature. A good understanding about their growth mechanism and bonding motifs is helpful to gain more insight into physicochemical characteristics of bulk materials. Following the first experimental observations by photoelectron spectroscopy (PES) carried out by Wang and co-workers,[8] small boron clusters have extensively been investigated by many research groups.[9]-[16] Let us briefly summarize the main results recently reported in the literature.

Using combined theoretical and experimental PES results, Wang and coworkers showed that there is an energetic competition between two-dimensional (2D) and three-dimensional (3D) structures of the anionic species B_{40}^-,[17] while smaller sized anionic clusters prefer 2D structures. More interestingly, the intermediate sized anionic clusters such as B_{30}^-,[15e] B_{35}^-,[18] B_{36}^-[19] and B_{40}^-[17] contain hexagonal holes as small defect boron sheets. While the anionic clusters B_n^- with n = 2-20 have quasi-planar structures that are completely composed of triangular units, larger clusters B_n^- with n = 21-25 tend to prefer 2D structures with five-membered holes.[15,16]

At the neutral state, it was found that the B_{40} size is an all-boron fullerene which is much more stable than 2D structures.[17]. The cluster B_{38} was proposed as a structural transition size due to the indistinguishable difference in energy between a 3D all-boron fullerene and a quasi-planar structure containing two hexagonal holes.[20,21]At smaller sizes, the neutral B_{36} was found to be a highly symmetrical structure with one central hexagonal hole,[19] and the neutral B_{30}[22] exhibits an aromatic bowled structure containing one central pentagonal hole. More recently, we interestingly found that the B_{32} cluster exhibits a bowled structure containing heptagonal hole[23] which is more stable than the tubular form previously reported. We should note that except for the cage-like B_{14} cluster,[14] small boron clusters B_n with n = 2 -19 have 2D structures that are formed on the basis of triangular B_3 units.[16]

PCCP RSCPublishing

Paper

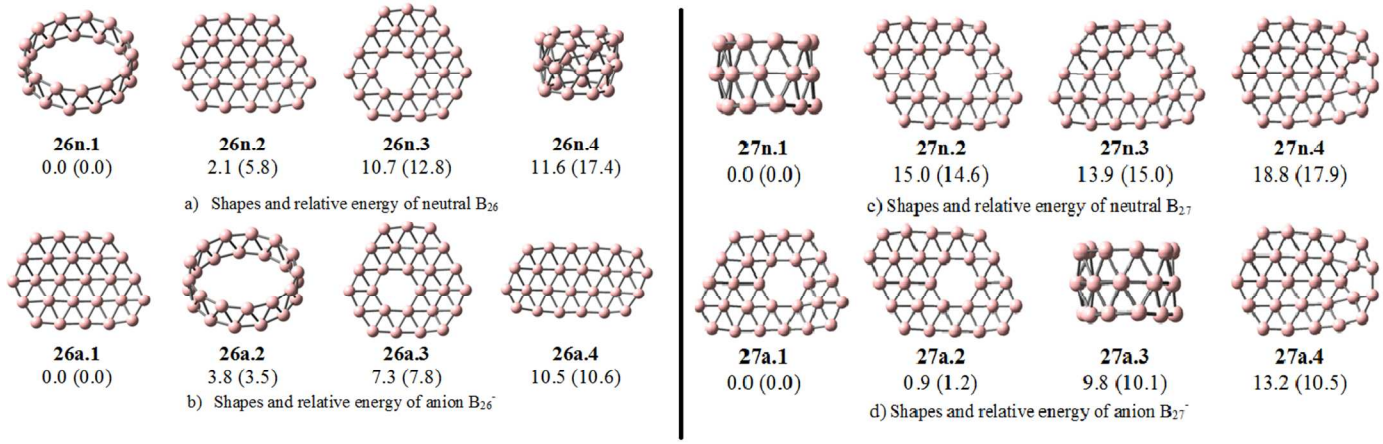

Fig. 1 Shapes and relative energy (kcal/mol) of the low-lying isomers of a) neutral B_{26}, b) anion B_{26}^-, c) neutral B_{27} and d) anion B_{27}^- obtained at CCSD(T)/6-311G(d)//PBE/6-311+G(d) and PBE/6-311+G(d) (in parenthesis)

Some special species such as B_{20},[24] B_{22}[12b] and B_{24}[25] were reported to have tubular forms in which two boron rings are connected together in antiprism bonding motif. More recently, Nguyen and co-workers[26] reported that the B_{27} has stable triple-ring shape composed of three nine-membered rings.

The structural landscape of small boron clusters $B_n^{0/-}$ with $n \leq 30$ were thus almost established, except for some sizes, namely the n = 23, 25, 26, 28 and 29 for neutral species and n = 26-29 for anionic species, that have not been investigated. Such a lack of data leads to the fact that a general view on the growth mechanism and structural characteristics of boron clusters is still missing. We should note that excepting some special species, including B_{11}, B_{16} and B_{17} whose structures were experimentally identified by the IR spectra,[15f] all remaining neutral species were only theoretically predicted by computational studies.

In this context, we performed and report in the present paper a theoretical study on the geometrical and electronic structure and photoelectron spectroscopy of boron clusters B_n including the sizes n = 26 ÷ 29, at both neutral and anionic states using DFT and MO computational methods. After determining the properties of these sizes, an overview of structural characteristics of boron clusters can be established on the basis of geometrical structures of known boron clusters. Thus, this report not only fulfil the missing gap of B_n clusters (n= 26 ÷ 29), but it also gives us more insight into a general growth mechanism of boron clusters.

Computational methods

All electronic structure calculations were carried out using the Gaussian 09[27] and Molpro 09[28] packages. Initial searches for all possible lower-lying isomers of B_{26-29} clusters were performed using a stochastic search algorithm that was implemented by us.[29] Firstly, the possible structures of the clusters considered were generated by a random kick method, and then rapidly optimized using density functional theory with the PBE functional[30,31] and the small 3-21G basis set. In this search procedure, the minimum and maximum distances between atoms were limited to 1.5 and 15 Å, respectively. Geometries of the local minima such located with relative energies lying in the range of 0.0 - 5.0 eV and their harmonic vibrational frequencies were further refined using the PBE functional but in conjunction with the larger 6-311+G(d) basis set.[32] Single-point electronic energies of the low-lying isomers obtained from PBE/6-311+G(d) computations were subsequently calculated using the coupled-cluster theory CCSD(T)[33,34] with the 6-311G(d) basis set. The photoelectron spectra of anionic clusters B_n^- were also simulated using time dependent DFT method, but with the same functional and basis set, TD-PBE/6-311+G(d).

Results and discussion

Searching the lower-lying isomers B_n with n = 26 - 29

In this section, we successively describe the structures of the clusters considered. For each size, both neutral and anionic forms are discussed. As for a convention, each structure is labelled by ***n*x.y** where ***n*** ranges from **26** to **29**, **x** stands for a neutral **n** or an anion **a,** whereas **y** denotes the ordering of the isomers (**1**, **2**…).

PCCP RSCPublishing

Paper

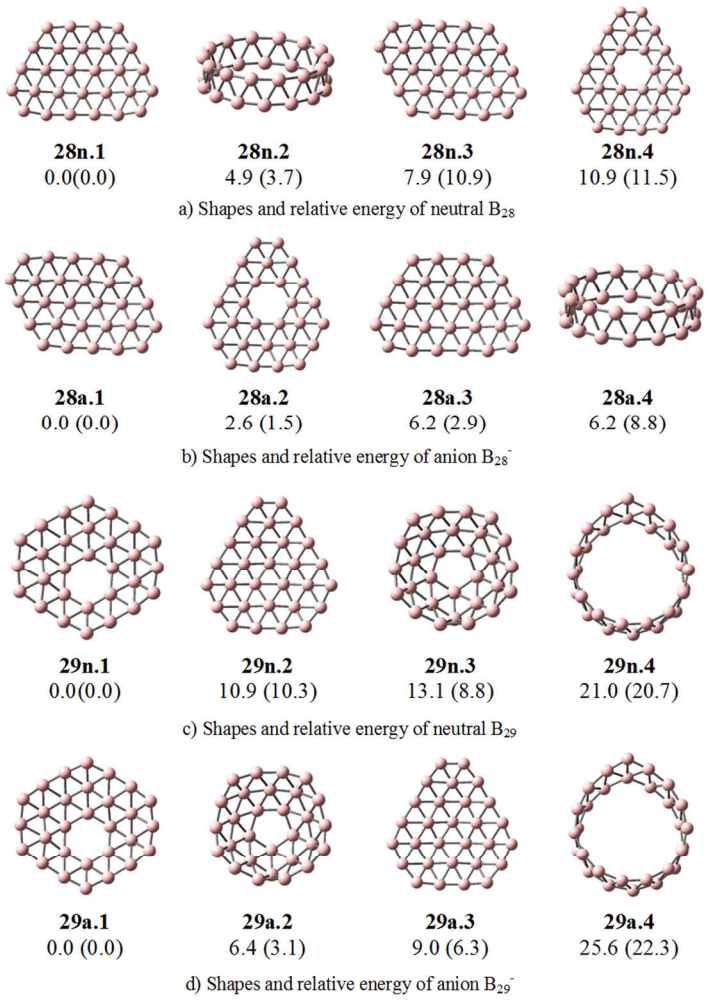

Fig. 2 Shapes and relative energy (kcal/mol) of the low-lying isomers of a) neutral B_{28}, b) anion B_{28}^-, c) neutral B_{29} and d) anion B_{29}^- obtained at CCSD(T)/6-311G(d)//PBE/6-311+G(d) and PBE/6-311+G(d) (in parenthesis)

Clusters $B_{26}^{0/-}$. Shapes and relative energies of the lower-lying isomers $B_{26}^{0/-}$ depicted in Figure 1a and 1b reveal that the double-ring tubular form **26n.1** (Ci, ^1A_g) is the most stable isomer of the neutral B_{26}. This structure is formed by connecting two 13-membered rings in an antiprism bonding motif and is similar to structural characteristic of the B_{20} and B_{24} clusters.[9,24] A quasi-planar structure **26n.2** (C_1, ^1A) is found to be the next isomer which is only 2.1 kcal/mol less stable than **26n.1** at the CCSD(T)/6-311G(d)//PBE/6-311+G(d) level.

Similar observations to smaller size clusters are found for the anionic state. The quasi-planar structures are more favourable, and the **26a.1** (C_1, ^2A) which is anionic form of **26n.2** is the most stable isomer of the anion B_{26}^-. The double ring form **26a.2** (C_i, ^2A_u) is the next isomer and 3.8 kcal/mol higher in energy as compared to **26a.1**. Although the structure containing hexagonal hole **26a.3** (C_1, ^2A) and other quasi-planar **26a.4** (C_1, ^2A) are located as local minima, they are 7.3 and 10.5 kcal/mol less stable than **26a.1**.

Clusters $B_{27}^{0/-}$. In agreement with previous report,[26] our CCSD(T) calculations show that the triple-ring form **27n.1** (C_1, ^2A) in which three nine-membered rings are connected together is the global minimum of the neutral B_{27} (Fig. 1c). Two 2D structures **27n.2** (C_1, ^2A) and **27n.3** (C_1, ^2A) have approximately similar energy levels and are 15.0 and 13.9 kcal/mol less stable than **27n.1**, respectively.

Interestingly, a reserved energy ordering is also found at the anionic state. Accordingly, both isomers **27a.1** (C_1, ^{1}A) and **27a.2** (C_1, ^{1}A) where each contains one hexagonal hole, are almost degenerate in energy and constitute the most stable isomers of B_{27}^- (Fig. 1d). These structures were missed in the previous report.[26] The triple ring form **27a.3** (C_1, ^{1}A) is 9.8 kcal/mol less stable than the **27a.1** at the CCSD(T)/6-311G(d) level. The structure **27a.4** (C_s, ^{1}A') that was reported to be the lowest-lying isomer by Duong *et al*.[26] turns out to be much less stable with a relative energy of 13.2 kcal/mol.

Clusters $B_{28}^{0/-}$. The shapes and relative energies of the lower-lying isomers of $B_{28}^{0/-}$ and $B_{29}^{0/-}$ are depicted in Fig 2. Interestingly, our calculations point out that the tubular form is no longer favourable for boron clusters B_n with $n \geq 28$. At the CCSD(T)/6-311G(d)//PBE/6-311+G(d) level, **28n.1** (C_s, ^{1}A') which is completely composed of triangular units, is now the global minimum of neutral B_{28}. The double ring form **28n.2** (C_{14}, ^{1}A) in which two 14-membered rings are connected together in antiprism bonding motif is the second isomer and is 4.9 kcal/mol less stable than **28n.1**. The quasi-planar structures **28n.3** (C_2, ^{1}A) and **28n.4** (C_s, ^{1}A') are of low-energy and lie 7.9 and 10.9 kcal/mol higher.

Following attachment of one excess electron into the neutral B_{28}, the anion B_{28}^- prefers the quasi-planar structures. According to our computed results, three lowest-lying isomers have 2D shapes. Both isomers **28a.1** (C_2, ^{2}A) and **28a.2** (C_1, ^{2}A) are almost degenerate with an energy gap of only 2.6 kcal/mol. **28a.3** (C_s, ^{2}A') which is the anionic form of **28n.1**, is found to be 2.9 and 6.2 kcal/mol higher in energy at the PBE/6-311+G(d) and CCSD(T)/6-311G(d), respectively. Consequently, these two isomers are expected to co-exist in experimental observations.

Clusters $B_{29}^{0/-}$. In a good agreement between DFT and CCSD(T) computed results, the isomer **29n.1** (C_1, ^{2}A) containing one hexagonal hole is the most stable isomer of B_{29}. This species can be considered as a fragment of the high symmetry cluster B_{36}. The second isomer is a quasi-planar structure **29n.2** (C_1, ^{2}A) which is formed by triangle B_3 units without any hole defect. **29n.3** (C_s, ^{2}A') which is formed by removing one B-atom from the bowl B_{30} is 13.3 kcal/mol higher in energy, while the double-ring **29n.4** (C_s, ^{2}A') is less stable. The global minimum **29n.1** can thus be considered as the smallest member of the family of boron clusters featuring hexagonal hole defect.

The global minimum of B_{29}^- anion is **29a.1** (C_1, ^{1}A) which is the anionic form of **29n.1**. Next isomers include **29a.2** (C_s, ^{1}A') and **29a.3** (C_s, ^{1}A') which are anionic species of **29n.3** and **29n.2**, respectively.

Vertical (VDE) and adiabatic (ADE) detachment energy.

The determination of VDE and ADE values of anionic boron clusters is important since these values are very useful to confirm the structural characteristics of anionic clusters. Let us note that structures of atomic clusters cannot directly be identified by common analytical experimental methods. On the other hand, they can indirectly be determined by using combined theoretical and experimental studies. Firstly, a theoretical exploration will be carried out to find the lowest-lying isomers located on the potential energy surface of each clusters. The theoretical spectrometry characteristics such as infrared (IR), photoelectron (PE) spectra of these isomers will then be computed and compared to the experimental spectra. The infrared (IR) spectrum is commonly used as fingerprint for the neutral and cationic clusters, while the photoelectron spectra are usually used for anionic clusters.

The vertical and adiabatic detachment energies and subsequently PE spectra of anionic clusters are simulated using TD-DFT methods. While the plots of predicted PE spectra are depicted in Fig. 3, their computed VDE values and corresponding final electronic configurations are given in Table S1-S6 of the Supplementary Information.

The first VDE of **26a.1** (C_1, ^{2}A) obtained by detaching one electron from its SOMO is equal to 3.71 eV and is somewhat larger than the ADE value of 3.57 eV (Fig. 3a). The energy gap between ADE and first VDE values is only 0.14 eV, indicating a msall geometry relaxation. The second VDE at 4.15 eV of **26a.1** comes from electron detachment from its HOMO-1 resulting in the first triplet state. Other peaks corresponding to several singlet and triplet states are observed in the range of 4.29 - 5.68 eV, as shown in Fig. 3a.

Because both anions **27a.1** (C_1, ^{1}A) and **27a.2** (C_1, ^{1}A) are almost degenerate with a tiny energy gap, we expect that both will appear in the PE spectrum of anion B_{27}^-. The simulated spectra of **27a.1** and **27a.2** shown in Fig. 3b and 3c reveal that there exhibit many intense peaks, very close to each other. The computed ADE and first VDE of **27a.1** are equal to 3.85 and 3.98 eV, respectively. They are slightly larger than corresponding values of ADE = 3.78 eV and VDE = 3.88 eV of **27a.2**. These first VDEs of both **27a.1** and **27a.2** come from electron detachment from their HOMOs. Similarly, the second VDE of both **27a.1** and **27a.2** originate from detaching one electron from their HOMO-1 and equal to 4.33 and 4.23 eV, respectively. Interestingly, we can observe that the third VDEs of **27a.1** and **27a.2** are almost overlapped (4.48 eV for the first, and 4.46 eV for the later) and correspond to an electron detachment from their HOMO-2. We expect that they will appear at the same peak with high intensity in the experimental spectrum. The remaining peaks are located in the range of 4.58 - 5.30 eV, and given in detail in Table S1 of Supplementary Information.

Similar to the case of the anionic B_{27} clusters, we also expect that both isomers **28a.1** (C_2, ^{2}A) and **28a.2** (C_1, ^{2}A) will be presented in the experimental spectra since they are almost degenerate with small energy gap of 2.6 kcal/mol at the CCSD(T)/6-311G(d) level (1.5 kcal/mol at PBE/6-311+G(d)). The first VDE at 3.68 eV of **28a.1** originates from electron detachment from its SOMO. This value is slightly larger than first VDE of 3.59 eV of **28a.2** in the same channel of electron detachment. For both isomers, detaching one electron from the HOMO-1 results in the first triplet state, and their second VDEs are 3.93 eV for **28a.1** and **4.12** eV for **28a.2**. Interestingly, it can be observed that the next five VDE values of **28a.1** and **28a.2** are very close to each other, and are expected to be presented in high intensity peaks of the experimental spectrum (Fig. 3d and 3e).

For the simulated PE spectrum of **29a.1** (C_1, ^{1}A), the first

VDE located at 3.62 eV arises from electron detachment from its HOMO and is close to the ADE value of 3.52 eV, due to small geometrical changes. The second VDE of **29a.1** at 4.00 eV corresponds to a detachment of one electron from its HOMO-2, while other intense peaks are located in a range of 4.47 -4.87 eV

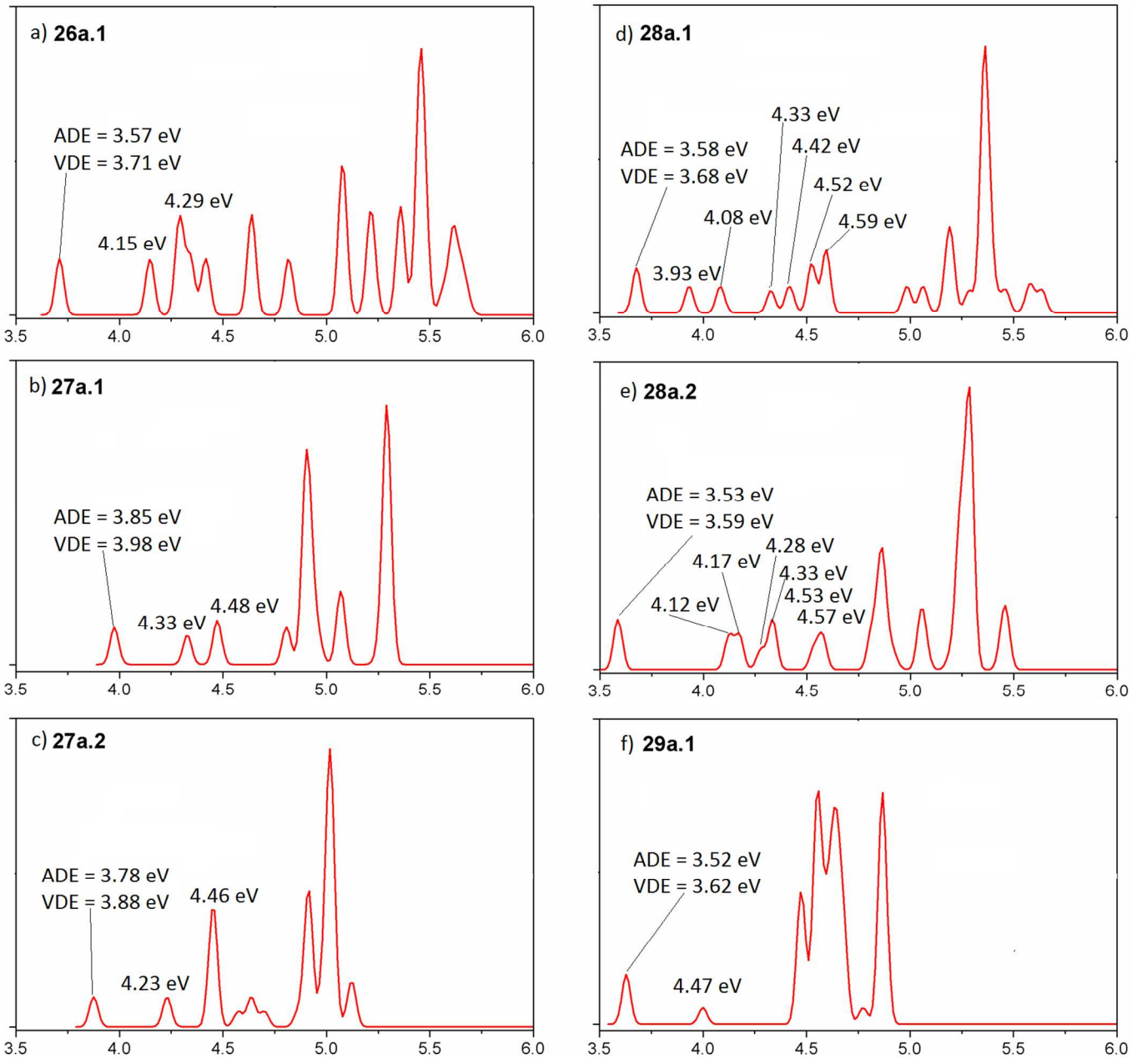

Fig. 3 Simulated PES of a) **26a.1**, b) **27a.1**, c) **27a.2**, d) **28a.1**, e) **28a.2** and f) **29a.1** obtained using TD-PBE/6-311+G(d) computations.

PCCP RSCPublishing

Paper

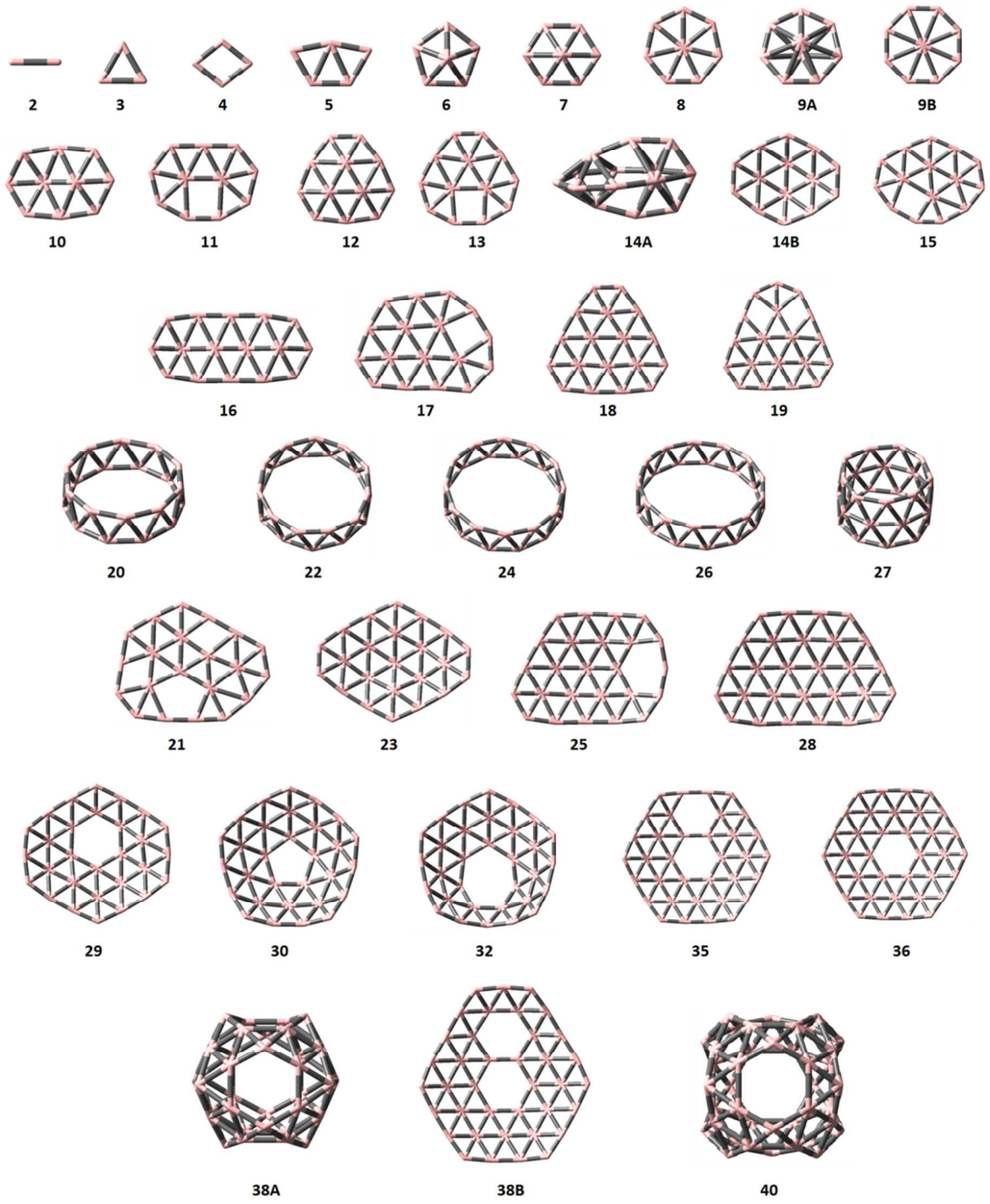

Fig. 4 Shapes of boron clusters B_n with n = 2-30 and 32, 35, 36, 38 and 40 obtained from refs. 16-23 and 35

PCCP RSCPublishing

Paper

An overview of structural characteristic and growth mechanism of boron clusters.

The unique structural characteristic is one of the most exciting features of small boron clusters. While atomic clusters of most elements exhibit three-dimensional geometrical structures, small boron clusters possess intriguing quasi-planar or planar structures. However, due to the fact that the earlier studies were commonly carried out on either one or a few special sizes, an overview of growth mechanism of boron clusters is missing. After determining the structures of the remaining sizes, we are now able to have a more global view.

For the sake of comprehension, we plot in Figure 4 the shapes of the B_n clusters actually known so far with certain accuracy. It can be observed that all small boron clusters B_n with n = 2 -40 are formed on the basis of triangle units in different arrangement motifs. We can separate them into several sub-groups:

a) Clusters B_n with n = 2 -5 are simply composed of triangle units.

b) Except for the B_9 and B_{14} sizes where the 3D structures **9A** and **14A** were determined as the global minima, and are somewhat more stable than the 2D structures **9B** and **14B**, respectively, the species B_n with n = 6 -19 are formed from the same triangular motif in which a small inside unit are stabilized by a larger outside ring. The inside unit of B_6-B_9 is simply one B-atom and it is replaced by larger unit such as diatomic B_2 unit for B_{10}-B_{11}, triangular B_3 unit for B_{12}-B_{13}, tetraatomic B_4 unit for B_{14}-B_{15}, pentaatomic B_5 unit for B_{16}-B_{17} and hexaatomic B_6 unit for B_{18}-B_{19}.

It is interesting that the anionic species B_n^- (n = 2÷19) exhibit quasi-planar and planar structures in an arrangement motif similar to those of the neutral species B_n.[15k] While small clusters B_n^- with n = 3 ÷ 6 are simply composed of triangle units, each of the larger sized clusters B_n^- with n = 7÷ 19 contains one small inside unit which is stabilized by a larger outside ring.

c) For the following species B_n with n = 20 -28, the growth motif is getting more complex. The species having an even electron number B_n ($n = 2m$ = 20, 22, 24 and 26) mostly exhibit tubular formed structures in which the two m-membered rings are connected to each other in an antiprism bonding fashion. It is worthy to note that these tubular structures were theoretical identified to be the highly stable isomers for anionic species B_n^- with n = 20, 22 and 24 at the CCSD(T) level of theory.[6,15b,15c,24] However, they were not detected in the experimental photoelectron spectra of anion B_{20}^-, B_{22}^- and B_{24}^-.[15b,15c,24] The reason for these controversies is unclear and it can come from either limit of computational approaches used or the experimental condition. We expect that the theoretical and experimental investigations will be further performed on these systems to gain more insight into these intriguing phenomena.

The B_{27} size is a special case and contains three 9-membered rings. Its bonding and aromatic characteristics was reported in a recent study.

The species B_{21}, B_{23}, B_{25} and B_{28} are formed on the basis of an inside B_6 unit surrounded by B-atoms. It can be seen that the B_{21} structure is a vacancy defect structure of the B_{23}. Similarly, the B_{25} is a vacancy defect structure of the B_{28}.

d) For the larger size clusters B_n with $n \geq 29$, the structures containing holes become more favourable. The B_{30} and B_{36} clusters are highly symmetrical structures which contain pentagonal and hexagonal holes, respectively. Remarkably, the B_{32} exhibits a bowled structure which contains a heptagonal hole. Other known structures such as B_{29} and B_{35} can be considered as defect species of these stable structures. The shape of B_{35} is similar to that of B_{36}, but one B-atom is removed. B_{29}can be regarded as one fragment of the B_{36}.

e) Recent studies showed that all-boron fullerenes B_n interestingly appear at n = 38 and 40. The fullerene form was determined as the global minimum of the B_{40} which is much stable than the quasi-planar structures. Two structures including a fullerene **38A** and a quasi-planar structure **38B** are almost degenerate on the energy landscape of the B_{38} system.

From the above overview of the structural characteristics, we can expect that the intermediate size boron clusters are likely formed by combining three main bonding motifs:

i) Quasi-planar structures contain the k-membered holes with k = 5 - 7. Larger holes with $k \geq 8$ are less stable, and thus they will presumably be less favourable.

ii) All-boron fullerenes will appear at some special sizes since low symmetry 3D structures tend to be less stable than the quasi-planar structures.

iii) Tubular structures will be expected to be stable structures at a few special sizes.

Let us note that although experimental confirmations have not been reported, all-boron fullerenes such as B_{80}, B_{92}…were theoretically proposed long time ago.[3,4] In addition, boron based nanomaterials such as boron nanosheets,[5,6,7] boron nanotubes[1,2] become intriguing subjects in the fields of materials science. More recently, the B_{84} cluster was also theoretically reported to exhibit a quasi-planar structure which contains four hexagonal holes.[36] It was proposed as a small fragment of β-boron nanosheet. These theoretical results give us more evidence that the all-boron nanomaterials are promising candidates for future experimental studies.

Conclusions

In the present work, we performed a theoretical study of geometrical and electronic structure of boron clusters B_n with n = 26 – 29) in both neutral and anionic states making use of quantum chemical DFT and MO methods. The photoelectron spectra of anionic species were simulated using TD-DFT methods. Our predictions showed that at the neutral state, the B_{26} and B_{27} clusters exhibit tubular forms, while the larger sizes B_{28} and B_{29} become quasi-planar structures. The anionic species B_n^- are more favourable in 2D shapes. More importantly, based on the geometrical characteristics of known boron clusters, we now established a general pattern of growth of boron clusters, which gives us more insight into the existence of boron based nanomaterials.

Acknowledgements

We are indebted to the KU Leuven Research Council (GOA program) and Vlaams Supercomputer Centrum (VSC). TBT would like to thank the FWO-Vlaanderen for a postdoctoral fellowship.

Notes and references

Department of Chemistry, University of Leuven, Celestijnenlaan 200F, B-3001 Leuven, Belgium.
E-mails: truong.batai@chem.kuleuven.be; minh.nguyen@chem.kuleuven.be
Electronic Supplementary Information (ESI) available: DOI: 10.1039/b000000x/

1 D. Ciuparu, R. F. Klie, Y. Zhu and L. Pfefferle, *J. Phys. Chem. B*, 2004, **108**, 3967.
2 F. Li, C. Shen, Z. Su, X. Ding, S. Deng, J. Chen, N. Xu and H. Gao, *J. Mater. Chem*., 2010, **20**, 2197.
3 (a) N. Szwacki, A. Sadrzadeh and B. I. Yakobson, *Phys. Rev. Lett*., 2007, **98**, 166804; (b) S. De, A. Willand, M. Amsler, P. Pochet, L. Genoverse and S. Grodecker, *Phys. Rev. Lett*, 2011, **106**, 225502.
4 Y. Li, G. Zhou, J. Li, B-L, Gu and W. Duan, *J. Phys. Chem. C*, 2008, **112**, 19268.
5 H. Tang and S. Ismail-Beigi, *Phys. Rev. Lett*, 2007, **99**, 115501.
6 T. B. Tai and M. T. Nguyen, *Chem. Eur. J*., 2013, **19**, 2942.
7 S. Er, G. A. Wijs and G. Brocks, *J. Phys. Chem. C*, 2009, **113**, 18962.
8 A. I. Boldyrev and L. S. Wang, *J. Phys. Chem. A*, 2001, **105**, 10759.
9 (a) I. Boustani, Z. Zhu and D. Tomanek, *Phys. Rev. B*,2011, **83**, 193405; (b) I. Boustani, *Chem. Modell*,, 2011, **8**, 1.
10 (a) J. Oscar, C. Jimenez-Halla, R. Islas, T. Heine and G. Merino, *Angew. Chem. Int. Ed*., 2010, **49**, 5668; (b) D. Moreno, S. Pan, L. L. Zeonjuk, R. Islas, E. Osorio, G. M. Guajardo, P. K. Chattaraj, T. Heine and G. Merino, *Chem. Commun*. 2014, **50,** 8140; (c) F. Cervantes-Navarro, G. Martinez-Guajardo, E. Osorio, D. Moreno, W. Tiznado, R. Islas, K. J. Donald amd G. Merino, *Chem. Commnun*., 2014, **50**, 10680
11 (a) S. R. Reddy and S. Mahapatra, *J. Chem. Phys*.,2012, **136**,024322; (b) S. R. Reddy and S. Mahapatra, *J. Chem. Phys*., 2012, **136**, 024323; (c) S. R. Reddy and S. Mahapatra, *J. Chem. Phys*., 2014, **140**, 084311
12(a) R. Casillas,, T. Baruah and R. R. Zope, Chem. Phys. Lett., 2013, 557, 15; (b) B. C. Hikmat, T. Baruah and R. R. Zope, *J. Phys. B: At. Mol. Opt. Phys*., 2012, **45**, 2255101.
13 E. Oger, N. R. M. Crawford, R. Kelting, P. Weis, M. M. Kappes and R. Ahlrichs, *Angew. Chem. Int. Ed*., 2007, **46**, 8503.
14 L. Cheng, *J. Chem. Phys*., 2012, **136**, 104301.
15 (a) Z. A. Piazza, W-L. Li, C. Romanescu, A. P. Sergeeva, L. S. Wang and A. I. Boldyrev, *J. Chem. Phys*., 2012, **136**, 104310; (b) A. P. Sergeeva, Z. A. Piazza, C. Romanescu, W-L. Li, A. I. Boldyrev and L. S. Wang, *J. Am. Chem. Soc*., 2012, **134**, 18065; (c) I. A. Popov, Z. A. Piazza, W. L. Li, L. S. Wang and A. I. Boldyrev, *J. Chem. Phys*., 2013, **139**, 144307; (d) Z. A. Piazza, I. A. Popov, W-L, Li, R. Pal, X. C. Cheng, A. I. Boldyrev and L. S. Wang, *J. Chem. Phys*., 2014, **141**, 034303; (e) W. L. Li, Y. F. Zhao, H. S. Hu, J. Li and L. S. Wang, *Angew. Chem*., 2014, **126**, 1; (f) C. Romanescu, D. J. Harding, A. Fielicke and L. S. Wang, *J. Chem. Phys.*, 2012, **137**, 014317; (g) A. N. Alexandrova, A. I. Boldyrev, H-J. Zhai and L-S, Wang, *Coord. Chem. Rev*. 2006, **250**, 2811 and references there in; (h) W. Huang, A. P. Sergeeva, H. J. Zhai, B. B. Averkiev, L. S. Wang and A. I. Boldyrev, *Nature Chemistry*, 2010, **2**, 202; (k) A. P. Sergeeva, I. A. Popov, Z. A. Piazza, W-L, Li, C. Romanescu, L-S. Wang and A. I. Boldyrev, *Acc. Chem. Res*., 2014, **47**, 1349
16 (a) A. G. Arvanitidis, T. B. Tai, M. T. Nguyen and A. Ceulemans, *Phys. Chem. Chem. Phys*. 2014, **16**,18311; (b) T. B. Tai, A. Ceulemans and M. T. Nguyen, *Chem. Eur. J*., 2012,**18**, 4510; (c) T. B. Tai, D. J. Grant, M. T. Nguyen and D. A. Dixon, *J. Phys. Chem. A*.,2010, **114**, 994; (d) T. B. Tai, N. M. Tam and M. T. Nguyen, *Chem. Phys. Lett*., 2012,**530**, 71; (e) T. B. Tai, N. M. Tam and M. T. Nguyen, *Theor. Chem. Acc*., 2012, **131**, 1241; (f) H. T. Pham, L. V. Duong, B. Q. Pham and M. T. Nguyen, *Chem. Phys. Lett*., 2013, **557**, 32; (g) H. T. Pham, L. V. Duong, N. M. Tam, M. P. Pham-Ho and M. T. Nguyen, *Chem. Phys. Lett*, 2014, **608**, 295.
17 H-J. Zhai, Y-F. Zhao, W-L. Li, Q, Chen, H. Bai, H-S. Hu, Z. A. Piazza, W-J. Tian, H-G. Lu, Y-B. Wu, Y-W. Mu, G-F. Wei, Z-P. Liu, J. Li, S-D. Li and L-S. Wang, *Nature Chem.*, 2014, **6**, 727.
18 W. L. Li, Q. Chen, W. J. Tian, H. Bai, Y. F. Zhao, H. S. Hu, J. Li, H. J. Zhai, S. D. Li and L. S. Wang, *J. Am. Chem. Soc*.,2014, **126**, 12257.
19 Z. A. Piazza, H-S. Hu, W-L. Li, Y-F. Zhao, J. Li and L-S. Wang, *Nature Commun.*, 2014, **5**, 3113.
20 J. Lv, Y. Wang, L. Zhu and Y. Ma, *Nanoscale*, 2014, **6**, 11692.
21 T. B. Tai and M. T. Nguyen, *Nanoscale*, 2015, **7**, 3316.
22 T. B. Tai, L. V. Duong, H. T. Pham, D. T. T. Mai and M. T. Nguyen, *Chem. Commun*., 2014,**50**, 1558.
23 T. B. Tai and M. T. Nguyen, *Chem.. Commun.* 2015,(**DOI:** 10.1039/C5CC01252J)
24 B. Kiran, S. Bulusu, H-J. Zhai, S. Yoo, X. C. Zeng and L. S. Wang, *PNAS*, 2005, **102**, 961.
25 S. Chacko, D. G. Kanhere and I. Boustani, *Phys. Rev. B*, 2003, **68**, 035414.

26 L. V. Duong, H. T. Pham, N. M. Tam and M. T. Nguyen, *Phys. Chem. Chem. Phys*, 2014, **16**, 19470.
27 M. J. Frisch *et al*., Gaussian 09, Revision C.01, Gaussian, Inc., Wallingford CT, 2009.
28 H. J. Werner, *et al*. MOLPRO 09, a package of ab initio programs, 2009.
29 T. B. Tai, M. T. Nguyen, *J. Chem. Theory Comput*. 2011, **7,** 1119.
30 J. P. Perdew, K. Burke and M. Ernzerhof, *Phys Rev Lett*., 1996, **77**, 3865.
31 J. P. Perdew, K. Burke and M. Ernzerhof, *Phys Rev Lett*., 1997, **78**, 1396.
32 J. A. Pople, *J. Chem. Phys*., 1980, **72**, 650.
33 M. Rittby and R. J. Bartlett, *J. Phys. Chem*., 1988, **92**, 3033.
34 P. J. Knowles, C. Hampel and H-J. Werner, *J. Chem. Phys*., 1994, **99**, 5219.
35 At the CCSD(T)/6-31G(d)//PBE/6-311+G(d) level of theory, we found that B_{23} and B_{25} are quasi-planar structures that are more stable than their tubular forms.
36 A. B. Rahane and V. Kumar, *Nanoscale*, 2015, **7**, 4055

A Table of Contents Entry

Electronic structure and photoelectron spectra of B_n with n = 26 – 29. An overview of structural characteristics and growth mechanism of boron clusters

Truong Ba Tai* and Minh Tho Nguyen*

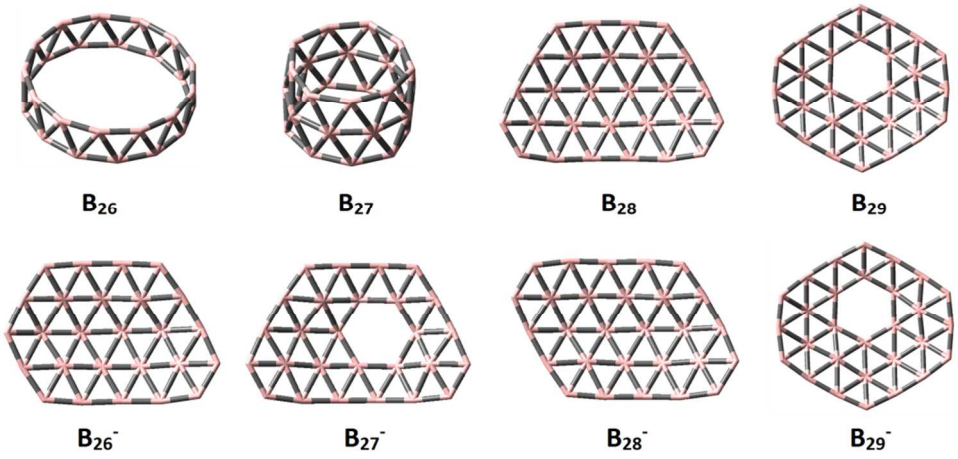

The most stable isomers of boron clusters B_{26-29} at neutral and anionic states

In this report, the electronic structure and photoelectron spectra of boron clusters B_{26-29} were theoretically investigated and an overview of growth mechanism of boron clusters was shown.